



Since January 2020 Elsevier has created a COVID-19 resource centre with free information in English and Mandarin on the novel coronavirus COVID-19. The COVID-19 resource centre is hosted on Elsevier Connect, the company's public news and information website.

Elsevier hereby grants permission to make all its COVID-19-related research that is available on the COVID-19 resource centre - including this research content - immediately available in PubMed Central and other publicly funded repositories, such as the WHO COVID database with rights for unrestricted research re-use and analyses in any form or by any means with acknowledgement of the original source. These permissions are granted for free by Elsevier for as long as the COVID-19 resource centre remains active.



Molecular modeling identification of potential drug candidates from selected African plants against SARS-CoV-2 key druggable proteins

J.O. Uhomoibhi, K.A. Idowu, F.O. Shode, S Sabiu*

Department of Biotechnology and Food Science, Faculty of Applied Sciences, Durban University of Technology (DUT), PO Box 1334, Durban, 4000, South Africa

ARTICLE INFO

Article history:

Received 4 February 2022

Revised 13 April 2022

Accepted 10 July 2022

Editor: DR B Gyampoh

Keywords:

Coronavirus disease 2019
Molecular dynamics simulations
Severe Acute Respiratory Syndrome
Coronavirus 2
Structural flexibility

ABSTRACT

Coronavirus disease 2019 (COVID-19) pandemic, caused by the Severe Acute Respiratory Syndrome Coronavirus-2 (SARS-CoV-2) is one of the major health threats the world has experienced. In order to stem the tide of the virus and its associated disease, rapid efforts have been dedicated to identifying credible anti-SARS-CoV-2 drugs. This study forms part of the continuing efforts to develop anti-SARS-CoV-2 molecules and employed a computational structure-activity relationship approach with emphasis on 99 plant secondary metabolites from eight selected African medicinal plants with proven therapeutic benefits against respiratory diseases focusing on the viral protein targets [Spike protein (Sgp), Main protease (Mpro), and RNA-dependent RNA polymerase (RdRp)]. The results of the molecular dynamics simulation of the best docked compounds presented as binding free energy revealed that three compounds each against the Sgp (VBS, COG and ABA), and Mpro (COR, QOR and ABG) had higher and better affinity for the proteins than the respective reference drugs, cefoperazone (CSP) and Nelfinavir (NEF), while four compounds (HDG, VBS, COR and KOR) had higher and favorable binding affinity towards RdRp than the reference standard, ramdesivir (RDS). Analysis of interaction with the receptor binding domain amino acid residues of Sgp showed that VBS had the highest number of interactions (17) relative to 14 and 13 for COG and ABA, respectively. For Mpro, COR showed interactions with catalytic dyad residues (His172 and Cys145). Compared to RDS, COR, HDG, VBS and KOR formed 19, 18, 17 and 12 H-bond and Van der Waal bonds, respectively, with RdRp. Furthermore, structural examination of the three proteins after binding to the lead compounds revealed that the compounds formed stable complexes. These observations suggest that the identified compounds might be beneficial in the fight against COVID-19 and are suggested for further *in vitro* and *in vivo* experimental validation.

© 2022 The Authors. Published by Elsevier B.V. on behalf of African Institute of Mathematical Sciences / Next Einstein Initiative.

This is an open access article under the CC BY-NC-ND license (<http://creativecommons.org/licenses/by-nc-nd/4.0/>)

* Corresponding author.

E-mail address: sabius@dut.ac.za (S. Sabiu).

Introduction

The Severe Acute Respiratory Syndrome Coronavirus 2 (SARS-CoV-2) (etiological agent of the coronavirus disease 2019 (COVID-19)) is the major pandemic the world is currently experiencing. As of February 1, 2022, a total of 379 203 159 confirmed cases with over 5 676 248 deaths have been reported worldwide (<https://coronavirus.jhu.edu/map.html>). SARS-CoV-2 has a positive sense, single-strand RNA genome of about 30,000 bp and belongs to the family *Coronaviridae* and genus *Betacoronavirus* [1].

To date, there is no medically authorized medication for COVID-19, albeit vaccines have been developed and approved for global use [2]. However, the inadequate and uneven distribution of the vaccines coupled with accompanied myths/false information has undermined their general acceptability and has necessitated the need to develop effective anti-COVID-19 therapeutics. Through drug repurposing, the currently available drugs and phytochemicals are being screened and evaluated against SARS-CoV-2 biological targets and the results have been impressive [3–6] with some leads already undergoing pre-clinical evaluations [5].

From the druggable targets in the development of novel drugs against SARS-CoV-2, the specialized proteins/enzymes responsible for its successful entry into a suitable host and subsequent replication are very important. The structural proteins [3-chymotrypsin like protease (main protease (Mpro)) and RNA-dependent RNA polymerase (RdRp)] together with the spike glycoprotein (Sgp) that make up the viral envelope are typical examples of SARS-CoV-2's specialized proteins and are vital for its infectivity and pathogenesis [7]. For instance, the viral Sgp controls the attachment of SARS-CoV-2 to the host cell and the attachment arises via the interaction between the receptor binding domain (RBD) of the Sgp with the human angiotensin-converting enzyme 2 (hACE-2) receptor [8]. The Mpro on the other hand is essential for processing viral polyproteins that are central to viral maturation and their subsequent infectivity [7,9], while the RdRp has been implicated in the replication and transcription stages of SARS-CoV-2 [10]. Owing to the fundamental role of these proteins in SARS-CoV-2 entry and replication, they are considered as vital therapeutic targets for drug discovery against COVID-19 [11]. Interestingly, studies have reported that the inhibition of these protein targets by novel compounds or existing conventional drugs could either effectively inhibit the replication of the virus or completely kill the virus. Bromhexine hydrochlorides was reported without severe adverse effects, and clinically effective against COVID-19 [12]. Another recent study specifically reported the inhibition of SARS-CoV-2's Sgp by clioquinol and its derivatives [13]. A combination of HIV-protease inhibitors (lopinavir/ritonavir) has also been demonstrated to effectively kill SARS-CoV-2 at the cellular level [14]. Furthermore, phytochemicals such as geraniin, curcumin, cyanidin-3-glucoside, and other existing drugs such as cefoperazone, zanamivir, indinavir, nelfinavir, saquinavir, and remdesivir have been reported to potentiate inhibitory effect on SARS-CoV-2's druggable structural proteins both in *in vitro* and *in silico* [6,15–20]. Molecular dynamics (MD) simulation, an advanced technique, has been proficiently used in designing novel compounds, either through re-purposing or as a general computer-aided drug design application [4,5]. This study forms part of the continuing efforts to develop anti-SARS-CoV-2 drugs and used a computational structure-activity relationship approach with emphasis on 99 plant secondary metabolites from selected eight African medicinal plants with proven therapeutic benefits against respiratory diseases and related infections (Table 1, Supplementary Table S1). The 99 investigated compounds were selectively mined through a thorough literature search and were subsequently subjected to computational modeling to generate lead compounds against Sgp, Mpro and RdRp of SARS-CoV-2.

Methods

Molecular docking and simulation

Proteins (SARS-CoV-2 Sgp, Mpro and RdRp) and compounds' preparation

The X-ray crystal structures of the viral Sgp (PDB ID: 6LZG), Mpro (PDB ID: 6LU7) and RdRp (PDB ID: 7BV2) were downloaded from RSCB Protein Data Bank [19,29]. The three proteins' structures were then set up on the UCSF Chimera v1.14 [30]. The structures of the proteins were prepared by deleting water molecules, nonstandard naming, protein residue connectivity. The missing atoms of side chains and protein backbone were added to the protein structure before the molecular docking. The drug, Nelfinavir (NEF), Remdesivir (RDS) and cefoperazone A (CSP) have been reported with remarkable inhibitory effect

Table 1

The selected plants and their uses in respiratory and related infections.

Plant	Use(s) against respiratory and related infection(s)	Reference(s)
<i>Leonotis leonurus</i>	Croup, common cold, asthma	[21]
<i>Ocimum gratissimum</i>	Influenza, bronchitis	[22]
<i>Tetradenia riparia</i>	Common cold, flu, bronchitis	[23]
<i>Abrus precatorius</i>	Common cold, bronchitis, pneumonia	[24]
<i>Artemisia afra</i>	Croup, flu, influenza	[25]
<i>Carapa procera</i>	Pulmonary diseases	[26]
<i>Alepleidea amatymbica</i>	Common cold, flu, influenza	[27]
<i>Drosera madagascariensis</i>	Croup, influenza	[28]

on the activities of SARS-CoV's Mpro, Sgp, and RdRp, respectively, and were used as reference inhibitors [17,20,31]. On the other hand, the 3-D structures of the selected 99 compounds (Supplementary Table S1) and the reference drugs (NEF, RDS and CSP) were prepared using Avogadro software v1.1.0.

Molecular docking

The Autodock Vina interface on Chimera, version 1.11 was used with default parameters for molecular docking [32,33]. Gasteiger charges were added to the compounds, and non-polar hydrogen atoms were added to carbon atoms follow by molecular docking. The compounds were docked at the active sites of Sgp, Mpro, and RdRp with grid box size (22 × 41 × 18), (76 × 68 × 74) and (112 × 104 × 92) pointing in x, y and z directions, respectively. Molecular dynamics (MD) simulation was done on the best docked compounds for Sgp (COG, VBS, and ABA) for Mpro (COR, QOR, and ABG) for RdRp (COR, HDG, VBS, and KOR) (Supplementary Table 1) and the reference drugs.

Molecular dynamic (MD) simulations

The MD simulation was performed as described by Kehinde *et al.* [34] with slight modification. The simulation was executed using the GPU version provided with the AMBER package (AMBER 18). In which the FF18SB variant of the AMBER force field was used to describe the systems. ANTECHAMBER was used to create atomic partial charges for the compounds by using the Restrained Electrostatic Potential (RESP) and the General Amber Force Field (GAFF) techniques. The Leap module of AMBER 18 permitted the addition of hydrogen atoms and chlorine ion (Cl⁻) counter ions to SARS-CoV-2's S_{gp} and sodium ion (Na⁺) to Mpro and RdRp, to neutralize all systems. All systems were then held implicitly inside an orthorhombic box of TIP3P water molecules such that all molecules were within 10Å of any box edge [35].

For both solutes 2000 steps initial minimization of were conducted with an applied restraint potential of 500 kcal/mol. They were executed for 990 steps utilizing the steepest descent method and followed by 990 steps of conjugate gradients. Additional 990 steps of full minimization were carried out employing the conjugate gradient algorithm (without restraint). Heating MD simulations from 0K to 300 K (gradual) were performed for 50 ps, such that the systems kept a fixed number of atoms and fixed volume. The systems' solutes have been imposed with a potential harmonic restraint of 10 kcal/mol and collision frequency of 1.0 ps. Afterward, an equilibration approximating 500 ps of each system was conducted; the operating temperatures were maintained at constant 300 K. Additional features for instance several atoms and pressure were also kept constant, imitating an isobaric-isothermal ensemble. The system's pressure was preserved at 1 bar utilizing the Berendsen barostat [36].

The entire time for MD simulations was 100 ns. For each simulation, the SHAKE algorithms were used to constrict hydrogen atoms' bonds [37]. The step size of each simulation was 2 fs, and an SPFP precision model was employed. The simulations matched with the isobaric-isothermal ensemble (NPT), with randomized seeding, the constant pressure of 1 bar retained by the Berendsen barostat [36], a pressure-coupling constant of 2 ps, a temperature of 300 K and Langevin thermostat [38] with a collision frequency of 1.0 ps.

Post-dynamic analysis and binding free energy calculations

Root mean square deviation (RMSD) and fluctuation (RMSF), radius of gyration (RG) analyses were done utilizing CPPTRAJ module used in the AMBER 18 suite. All plots were generated make use of the Origin data analysis software [39].

For the evaluation and assessment of the systems' binding affinity, the free binding energies were estimated using the Molecular Mechanics/GB Surface Area method (MM/GBSA) [40]. Binding free energies were averaged over 99000 snapshots extracted from the 99 ns trajectory. Equations below represent the method for the calculation of the free binding energy (ΔG) for each molecular species (complex, ligand, and receptor):

$$\Delta G_{\text{bind}} = G_{\text{complex}} - G_{\text{receptor}} - G_{\text{ligand}} \quad (1)$$

$$\Delta G_{\text{bind}} = E_{\text{gas}} + G_{\text{sol}} - TS \quad (2)$$

$$E_{\text{gas}} = E_{\text{int}} + E_{\text{vdw}} + E_{\text{ele}} \quad (3)$$

$$G_{\text{sol}} = G_{\text{GB}} + G_{\text{SA}} \quad (4)$$

$$G_{\text{SA}} = \gamma \text{SASA} \quad (5)$$

E_{gas} indicates the gas-phase energy, which consists of the internal energy E_{int} , Coulomb energy E_{ele} and the van der Waals energies E_{vdw} . The E_{gas} was directly estimated from the FF14SB force field terms. Solvation free energy, G_{sol} , was calculated from the energy contribution from the polar states, GGB, and non-polar states, G. The non-polar solvation energy, SA. The GSA was defined from the solvent-accessible surface area (SASA), using a water probe radius of 1.4 Å. In distinction, the polar solvation, GGB, the contribution was calculated by solving the GB equation. S and T represent the total entropy of the solute and temperature, respectively.

Table 2
Thermodynamic Binding Energy Profiles for the ligands towards SARS-CoV-2 Sgp.

Energy Components (kcal/mol)				
Spike Complex	Cefoperazone A (CSP)	Cyanidin-3-O-Glucoside (COG)	Verbasoside (VBS)	Abrusoside A (ABA)
ΔE_{vdw}	-41.342±4.214	-39.134±3.233	-36.454±3.334	-27.565±2.211
ΔE_{elec}	-12.343±1.545	-14.244±2.214	-13.455±2.102	-6.355±0.124
ΔC_{gas}	-29.344±3.214	-31.342±3.347	-40.245±4.321	-36.366±1.245
ΔC_{solv}	10.432±1.871	9.345±1.252	9.244±0.865	8.656±1.001
ΔC_{bind}	-31.847±3.588	-32.042±3.364	-34.785±4.248	-30.944±2.485

Table 3
Thermodynamic Binding Energy Profiles for the ligands towards SARS-CoV-2 Mpro protein.

Energy Components (kcal/mol)				
Mpro Complex	Nelfinavir (NEF)	Cyanidin 3-O-Rutinoside (COR)	Quercetin 3-O-Rutinoside (QOR)	Abrispogonol G (ABG)
ΔE_{vdw}	-41.134±3.214	-45.356±5.145	-40.234±1.289	-62.344±5.987
ΔE_{elec}	-14.456±2.121	-19.345±3.285	-18.344±0.598	-23.535±4.545
ΔC_{gas}	-52.455±5.325	-64.456±4.879	-49.344±4.587	-70.345±4.898
ΔC_{solv}	13.455±2.113	21.452±2.777	15.345±2.785	20.453±2.784
ΔC_{bind}	-45.847±3.588	-51.354±5.45	-48.709±6.283	-54.064±7.525

Table 4
Thermodynamic Binding Energy Profiles for the ligands towards SARS-CoV-2 RdRp protein.

Energy Components (kcal/mol)					
RdRp	Remdesivir (RDS)	Cyanidin 3-O-Rutinoside (COR)	Hederagenin (HDG)	Verbasoside (VBS)	Kaempferol-3-O-Rutinoside (KOR)
ΔE_{vdw}	-63.484±6.325	-74.274±3.121	-56.395±4.654	-75.766±5.545	-61.645±2.450
ΔE_{elec}	-34.485±4.215	-43.184±2.212	-32.454±1.895	-41.654±6.011	-34.444±3.214
ΔC_{gas}	-72.748±3.956	-81.35±7.212	-56.245±7.211	-44.754±3.232	-21.679±4.545
ΔC_{solv}	23.485±1.995	18.745±3.211	15.324±2.321	11.867±2.001	8.645±1.021
ΔC_{bind}	-42.847±3.588	-51.354±5.45	-48.709±6.283	-54.064±7.525	-48.601±4.927

Results and discussion

The results of the molecular docking for all the 99 compounds and the reference drugs for each target are shown in supplementary Table S1. After molecular docking analyses, the results of the binding affinities of the best docked compounds relative to the standards towards Sgp, Mpro, and RdRp, calculated as binding energy after being subjected to MD simulation of 100 ns trajectories are presented in supplementary Tables S2, S3 and S4, respectively. Compounds with higher or relatively close binding free energy values were considered to be lead compounds.

For the MD simulation, the results of the binding energies of the compounds against Sgp revealed that VBS and COG had higher binding affinities of -34.785 kcal/mol and -32.042 kcal/mol, respectively, while ABA had a relatively close binding energy value of -30.944 kcal/mol, when compared with CSP, -31.847 kcal/mol (Table 2). This finding suggests that the three compounds might be potent inhibitors of Sgp. From the Mpro enzyme complexes (Table 3), COR, QOR and ABG showed better binding energies than the reference drug, NEF. ABG exhibited the highest binding energy of -54.064 kcal/mol, with COR and QOR exhibiting binding energies of -51.354 kcal/mol and -48.709 kcal/mol, respectively. The result showed the three compounds had stronger binding interactions with Mpro, and possibly be potent and promising Mpro inhibitors. Inhibition of the Mpro enzyme is key for processing the polyproteins translated from RNA molecules of SARS-Cov-2 [9].

Table 4 presents the binding energy profiles of RdRp bound complexes with COR, HDG, VBS and KOR exhibiting higher binding energies than the reference standard, RDS (-42.847 kcal/mol), with VBS having the highest binding energy (-54.064 kcal/mol) relative to others. The high binding energy values observed with these compounds could be suggestive of better affinity towards RdRp and an indication of their inhibitory potential on RdRp as an attractive druggable target in the design of SARS-CoV-2 therapeutics. Interestingly, it is evident from this study that COR might be a promising and dual inhibitor of RdRp and Mpro, while VBS was identified as a dual inhibitor of Sgp and RdRp. The viral Mpro and RdRp play significant biological functions that are key for polyproteins' proteolytic processes and viral replication, therefore they are promising targets in the therapy of viral diseases [41]. Wu et al. [11] reported that majority of prospective anti-COVID 19 drug candidates are inhibitors of either protease or RdRp.

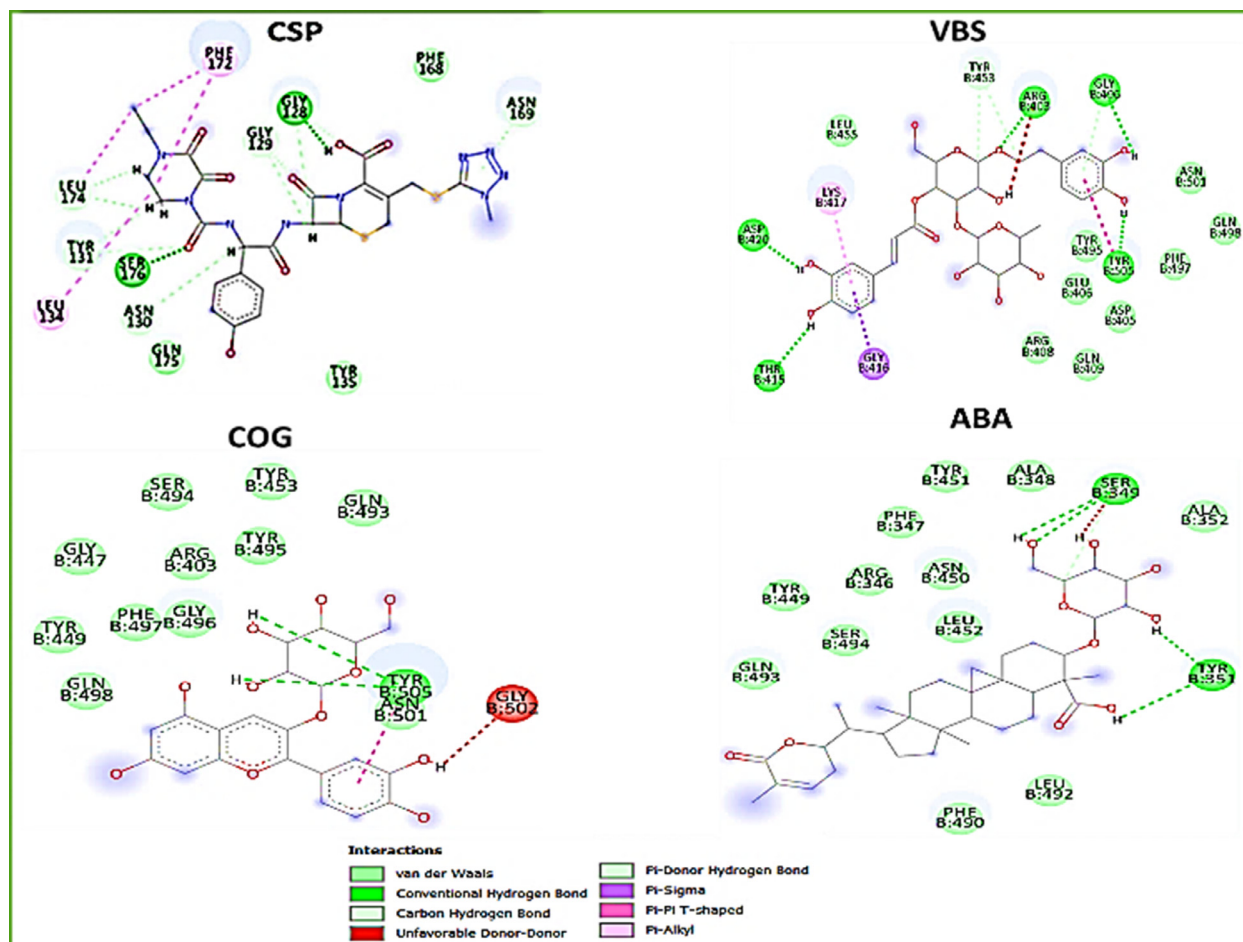


Fig. 1. 2D interaction plots of SARS-CoV-2's active site amino acid residues of Spike protein with CSP, VBS, COG, and ABA.

Interaction plots of the lead compounds with the viral structural proteins

Studies have used protein-ligand interaction plots to analyze interactions among the amino acid residues at the active sites of proteins and bound molecules [42,43]. In this study, the interactions established between the lead molecules and the amino acid residues at the active site of the respective target protein are presented in Figs. 1–3. Interactions such as hydrogen bond (H-bond), π -sigma, π -anion, π -Sulfur, alkyl, π -alkyl, amide- π stacked interaction, π - π , T-shaped interactions and Van der Waals (vdW) overlaps were observed between the ligands and the proteins. Specifically, VBS had the highest number of interactions (17) with the RBD amino residues of Sgp relative to 14 and 13 for COG and ABA, respectively.

All the three compounds with better binding affinity showed higher number of interactions than the reference drugs with total interaction number of 10. Similar to the reference drug, in addition to the H-bonds observed with all the lead compounds, one π -anion interactions with Gly 416 was observed with VBS, which might justify the observed higher binding energy with the two complexes in this study. The π -anion interaction has been reported to exist between promising inhibitors of SARS-CoV-2's Sgp and the RBD amino acid residues [44]. The π interactions and higher binding energy observed with VBS might be suggestive of its better potency than the other investigated compounds. Similarly, the interaction plots for the Mpro complexes are shown in Fig. 2. The proteases of coronaviruses are often referred to as Cys-His catalytic dyad due to the role of both His41 and Cys145 residues at their active site in biological catalysis [45]. Findings have shown that these residues are essential in Mpro inhibition, and possible interactions of potent inhibitor might result in the inhibition of coronaviruses Mpro [42,46]. In this study, the reference drug, NEF has 16 interactions and interacted with the active site His172 and Cys145 residues than the other ligands. Compound COR established 11 molecular interactions with binding site residues of Mpro and interacted with His 172, and this could be a tenable reason for its higher binding affinity towards the protein relative to the other two compounds. This observation was further supported by a previous report [43], where interaction with His172 amino residue of Mpro was considered vital for the inhibition of the specific activity of SARS-CoV-

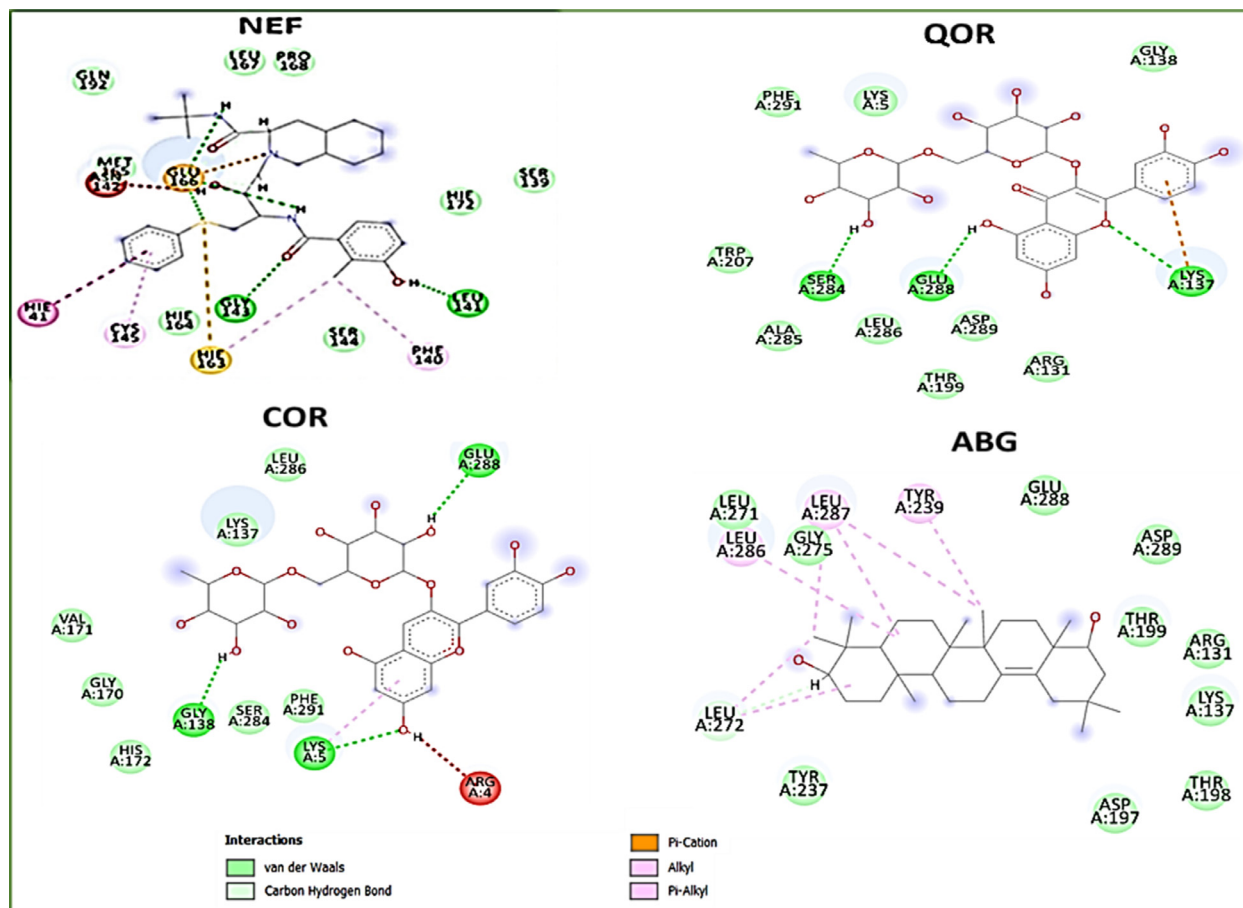


Fig. 2. 2D interaction plots of SARS-CoV-2's Mpro amino acid residues with NEF, QOR, COR and ABG.

2's Mpro. However, compounds QOR and ABG showed no interactions with neither His172 nor Cys145 residues, but more hydrogen interactions were observed in ABG (9) and QOR (11) than COR (7) and the reference drug (8). This finding and the result of the binding energy might suggest that the two compounds possibly inhibit Mpro through a different mechanism.

As shown in Fig. 3, RDS formed a total of 9 H- and Van der Waal bonds (Val 557, Ser 682, Ala 688, Thr 687, Asn 691, Asp 623, Cys 622, Asp 760, Lys 545) with RdRp active site amino residues alongside one Pi-cation interaction with Arg 555. A similar study [47] revealed that Ivermectin and remdesivir formed H-bond interaction with RdRp but inhibit RdRp through different mechanisms. Compared to RDS, COR, HDG, VBS and KOR formed 19, 18, 17 and 12 H-bond and van der Waal bonds, respectively with the protein. Furthermore, more pi interactions were formed in the tested compounds than the reference standard and these observations could both be supportive of their relatively higher affinities for the protein and suggestive their stronger inhibitory effect towards RdRp.

Dynamic stability and flexibility of Sgp-, Mpro-, and RdRp- bound and unbound complexes

The results of the post-MD simulation analyses presented as RMSD, RoG and RMSF as functions of structural stability, flexibility and compactness of the resulting complexes following ligands' binding on the respective proteins are shown in Figs. 4–6 and Tables 5–7. The binding of COG (2.211 Å), ABA (2.201 Å) and the reference drug, CSP (2.233 Å) on the RBD of Sgp slightly lowered the RMSD value when assessed to the unbound Sgp with an average value of 2.304 Å (Fig. 4, Table 5). This finding revealed the binding of the ligands stabilizes the protein structure. For all the compounds, their binding slightly raises the RMSD values, however, the relatively low RMSD values revealed the complexes are stable as all the values are less than 3.5 Å. This structural stability finding further support the hypothesis that these compounds might be good and promising inhibitor of Sgp of SARS-CoV-2.

The RMSD plots for the Mpro complexes revealed that the binding of all the ligands, NEF, COR, QOR and ABG brought more structural stability to the complexes (Fig. 5 and Table 6). This is evidenced from the lower average RMSD values of 1.679 Å, 2.164 Å, 2.132 Å and 2.127 Å, for NEF, COR, QOR and ABG, respectively, relative to 2.487 Å for the unbound Mpro. A similar decrease in RMSD value was reported after the binding of ligands such as cyanidin 3-glucoside and α-ketoamide-11r,

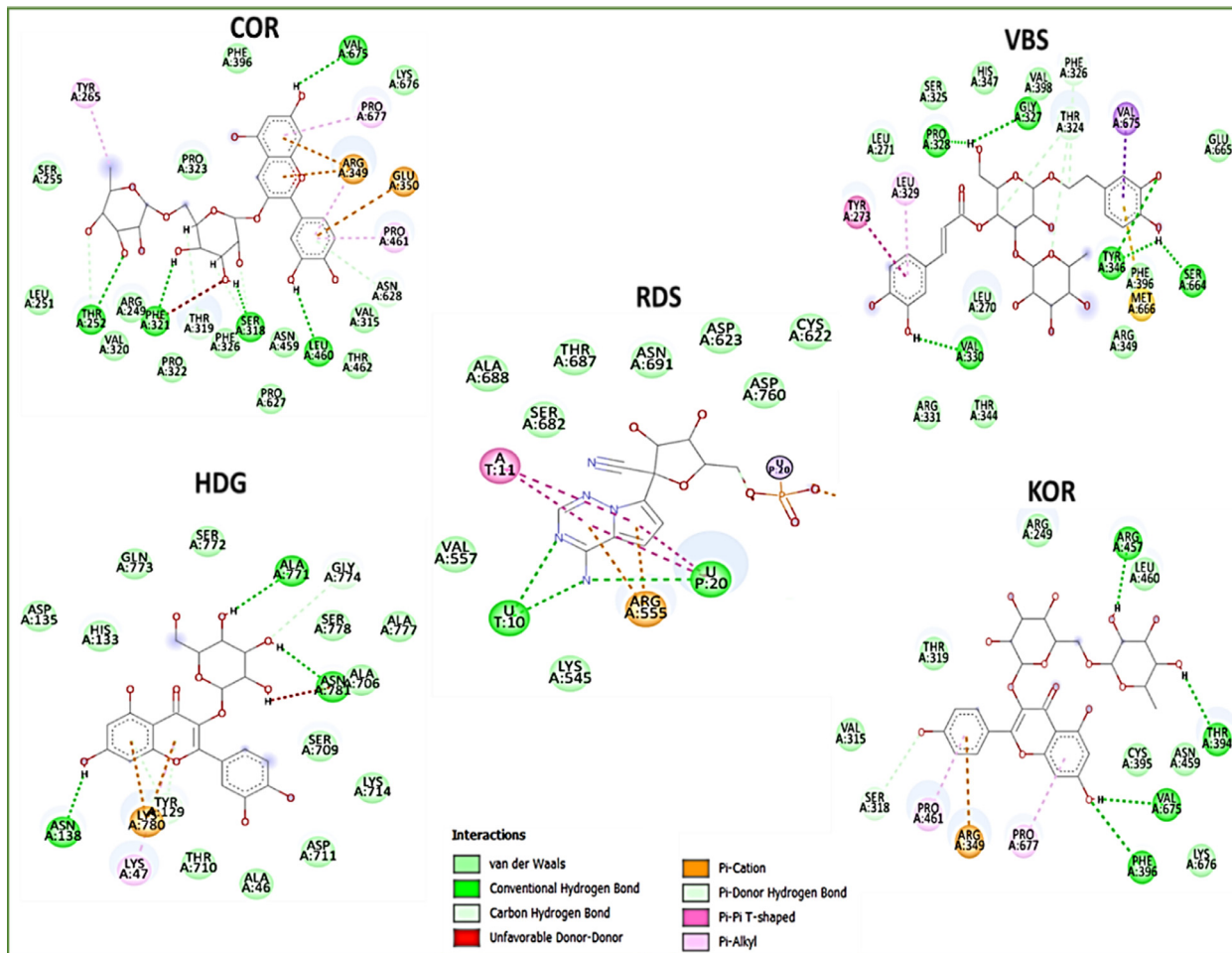


Fig. 3. 2D interaction plots of SARS-CoV-2's RdRp amino acid residues with RDS, COR, VBS, HDG and KOR.

Table 5

Calculated average values of parameter used to interpret structural stability and compactness of SARS-CoV-2's Sgp complexes.

Average Values			
Complex	RMSD (Å)	RoG (Å)	RMSF (Å)
Spike	2.304±0.340	17.243±1.533	1.213±0.056
Spike + CSP	2.233±0.045	18.921±1.954	1.461±0.085
Spike + VBS	2.891±0.353	19.217±2.032	1.732±0.242
Spike + COG	2.211±0.009	17.676±2.452	1.843±0.134
Spike + ABA	2.201±0.056	17.538±1.595	1.321±0.045

Table 6

Calculated average values of parameter used to interpret structural stability and compactness of SARS-CoV-2's Mpro complexes.

Average Values			
Complex	RMSD (Å)	RoG (Å)	RMSF (Å)
Mpro	2.487±0.008	20.625±2.442	1.461±0.904
Mpro + NEF	1.679±0.130	20.813±1.922	2.112±0.452
Mpro + COR	2.164±0.078	21.267±2.004	1.983±0.004
Mpro + QOR	2.132±0.156	20.899±0.989	1.601±0.153
Mpro + ABG	2.127±0.039	21.198±1.940	1.563±0.234

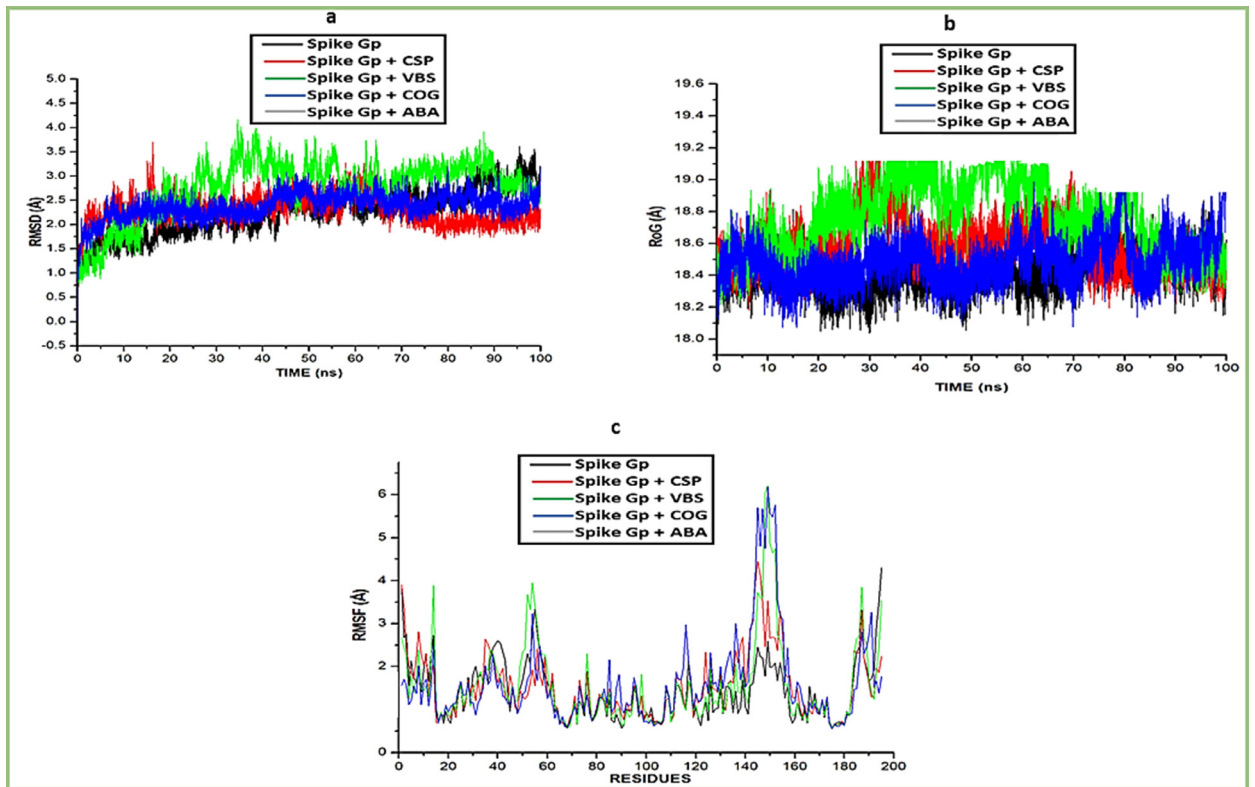


Fig. 4. Comparative profile plots of C- α atoms of SARS-CoV-2's spike protein with CSP, VBS, COG and ABA shown as a), RMSD b), RoG, and c). RMSF.

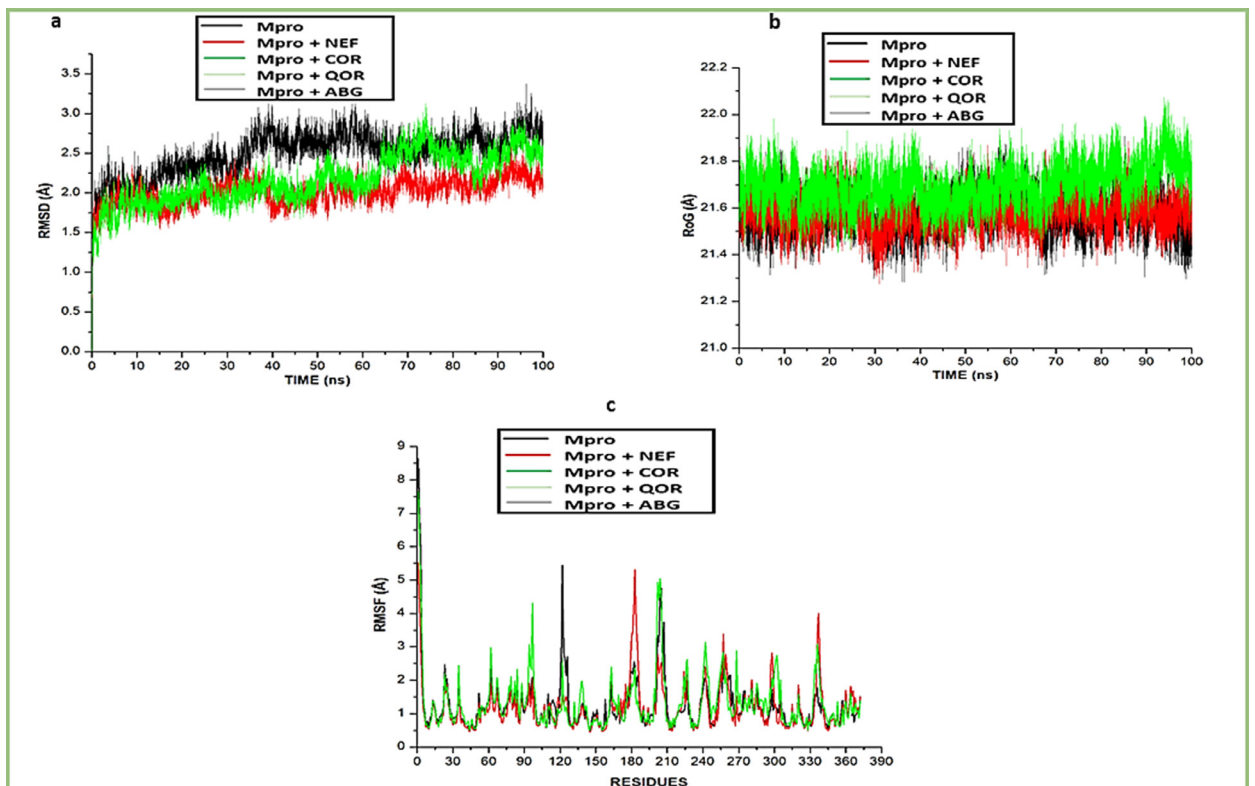


Fig. 5. Comparative profile plots of C- α atoms of SARS-CoV-2's Mpro with NEF, COR, QOR and ABG shown as a), RMSD b), RoG, and c). RMSF.

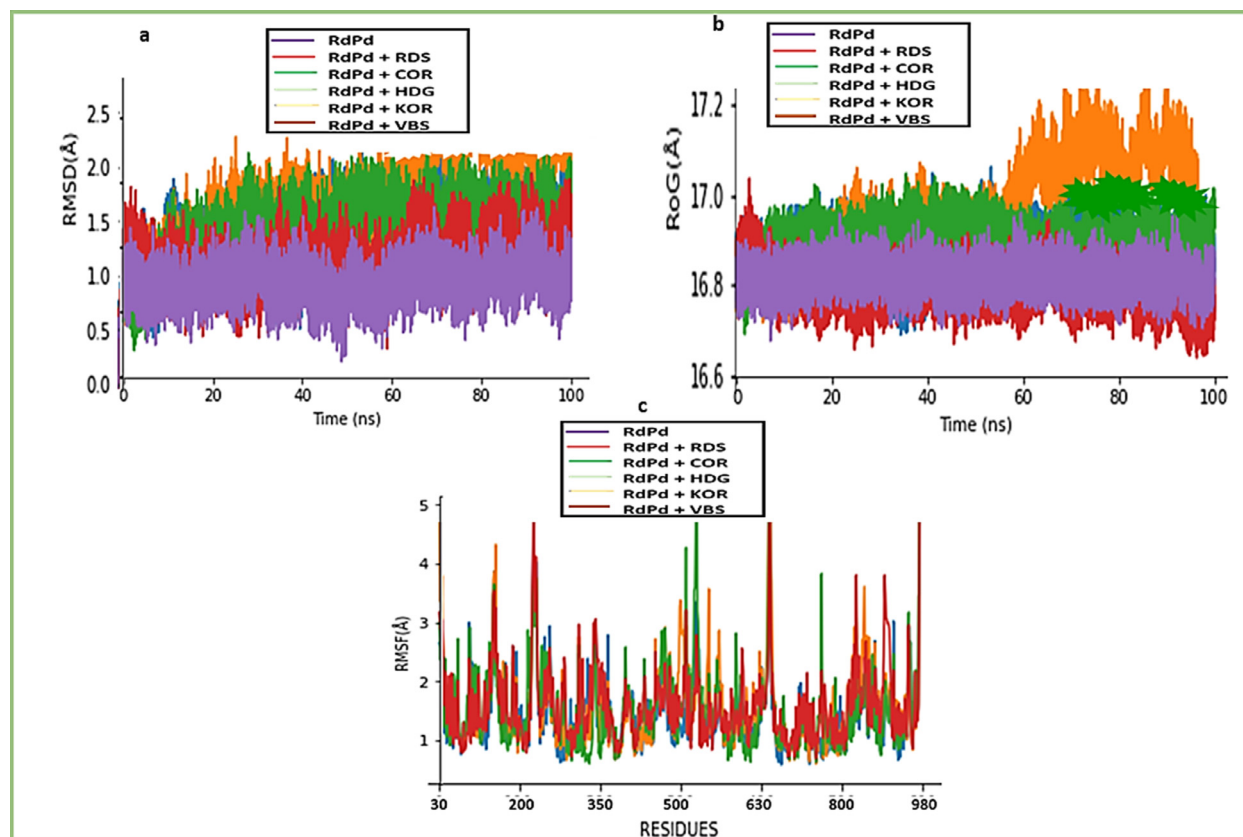


Fig. 6. Comparative profile plots of C- α atoms of RdRp enzyme with RDS, COR, HDG, KOR and VBS shown a). RMSD b). RoG, and c). RMSF.

Table 7

Calculated average values of parameter used to interpret structural stability and compactness of SARS-CoV-2's RdRp complexes.

Average Values			
Complex	RMSD (Å)	RoG (Å)	RMSF (Å)
RdRp	1.237 \pm 0.024	16.341 \pm 1.002	1.783 \pm 0.173
RdRp+ RDS	1.583 \pm 0.493	16.352 \pm 1.034	2.042 \pm 0.009
RdRp + COR	1.607 \pm 0.084	16.841 \pm 0.493	2.133 \pm 0.200
RdRp+ HDG	1.631 \pm 0.043	16.751 \pm 1.212	1.978 \pm 0.103
RdRp + KOR	1.806 \pm 0.043	17.393 \pm 0.984	2.231 \pm 0.064
RdRp + VBS	1.563 \pm 0.032	16.841 \pm 0.843	2.004 \pm 0.038

suggesting the ligand binding might change the protein conformation [43]. From the forgoing, it can be deduced that the binding of the ligands does not compromise the structural integrity of SARS-CoV-2's Mpro and suggestive of the ligands as potential inhibitors for the enzyme. However, a different trend was observed with the RdRp complexes, where binding of the compounds and the reference drug, RDS marginally raised the average RMSD values relative to the unbound enzyme but still within the acceptable limit of 2.5 Å [48] (Fig. 6, Table 7), and this could suggest a relative adjustment or change in structural conformation of the RdRp protein. This result corroborates a previous finding [49] that showed relatively low RMSD value after ligands (natamycin and leucal) bind to RdRp.

The RoG evaluates the structural solidity/compactness of proteins/receptors after binding of ligands and any significant alteration to the protein compactness induced by binding of ligands might affect the biological activity of the protein [50]. A lower RoG value indicates a more stable system [44]. In the three protein systems in this study, the binding of the lead compounds and reference drugs slightly raised the average RoG values compared to the unbound protein complexes (Figs. 4–6, Tables 5–7). For the Sgp, binding of CSP, VBS, COG and ABA relatively raised the average RoG values to 18.921 Å, 19.217 Å, 17.676 Å and 17.538 Å, respectively, relative to 17.243 Å for the unbound Sgp (Table 5), while it was 20.813 Å, 21.267 Å, 20.899 Å and 21.198 Å for NEF, COR, QOR and ABG, respectively compared to the apo- Mpro system (20.625 Å) (Table 6). Similar increase in average RoG values was also observed with binding of COR, KOR, VBS, HDG and RDS on the

RdRp system (Table 7) and these findings are not unusual, as studies [6,44] have similarly reported slight increase in RoG values after ligand binding and more importantly that the changes were only marginal and not statistically significant.

The RMSF measures the behavioral impact of the binding of molecules on the active site residues of a protein [51]. High and low fluctuation values suggest more and less flexible movements of the binding site residues, respectively. The binding of the ligands and the reference drug to the RBD of Sgp increased the average RMSF values compared to the unbound Sgp system (1.213 Å) (Table 5). For the Mpro system, the highest average RMSF value was observed with NEF (2.112 Å), followed by COR (1.983 Å), QOR (1.601 Å), ABG (1.865 Å) and the unbound protein (1.461 Å) (Table 6), and this was similarly consistent for the RdRp complexes (Table 7). Generally, the observations with respect to RMSF in this study revealed that binding of the lead ligands brought more flexibility to the overall protein structures in each case and are consistent with a previous study [52]. While this corroborates the observed marginally increased average RoG values in this study, it is also a further attestation to the inhibitory potential of the study compounds towards the respective protein systems as they have compared favorably with the respective reference standards.

Conclusion

The targeted SARS-CoV-2 proteins (Sgp, Mpro and RdRp) in this study are required and vital for viral entry and subsequent replication in human hosts and have been identified as therapeutic targets for development of drugs against COVID-19. Successful inhibition of these proteins will ultimately lead to reduction in the infectivity and replication of SARS-CoV-2. In this study, three compounds each demonstrated better or favorable binding affinity against Sgp and Mpro relative to the respective reference drugs, while four compounds (COR, HDG, KOR and VBS) demonstrated higher affinity or competed well with the reference standard towards, RDS for RdRp. A further probe into the structural stability, flexibility and compactness of the three proteins following binding of the lead compounds revealed formation of stable complexes with the proteins. While multiple parallel simulations might give possible statistical significance on the simulation runs, the overall findings from the single-trajectory simulations in this study suggests that the identified compounds might be beneficial in the fight against COVID-19 and are recommended for further *in vitro* and *in vivo* experimental validation. mmc1.docx

Declaration of Competing Interest

The authors declare that they have no known competing financial interests or personal relationships that could have appeared to influence the work reported in this paper.

Acknowledgments

The authors specially acknowledge the financial assistance of the Directorate of Research and Postgraduate Support, Durban University of Technology, and the Centre for High Performing Computing (CHPC), Cape Town, South Africa for providing the computing platform for this study. Research reported in this publication was also supported by the South African Medical Research Council (SA MRC) under a Self-Initiated Research Grant to S. Sabiu. The views and opinions expressed are those of the authors and do not necessarily represent the official views of the funders.

Supplementary materials

Supplementary material associated with this article can be found, in the online version, at doi:[10.1016/j.sciaf.2022.e01279](https://doi.org/10.1016/j.sciaf.2022.e01279).

References

- [1] L. Zou, F. Ruan, M. Huang, L. Liang, H. Huang, Z. Hong, J. Yu, M. Kang, Y. Song, J. Xia, L. M. Peiris, J. Wu, SARS-CoV-2 viral load in upper respiratory specimens of infected patients, *N. Engl. J. Med.* 382 (2020) 1177–1179.
- [2] G.M. Lee, The importance of context in Covid-19 vaccine safety, *N. Engl. J. Med.* 385 (2021) 1138–1140.
- [3] A.T. Jamiu, C.E. Aruwa, I.A. Abdulakeem, A.A. Ajao, S. Sabiu, Phytotherapeutic evidence against coronaviruses and prospects for COVID-19, *Pharmacogn. J.* 12 (2020).
- [4] S.K. Konstantinidou, I.P. Papanastasiou, Repurposing current therapeutic regimens against SARS-CoV-2, *Exp. Ther. Med.* 20 (2020) 1845–1855.
- [5] X. Yao, F. Ye, M. Zhang, C. Cui, B. Huang, P. Niu, X. Liu, L. Zhao, E. Dong, C. Song, In vitro antiviral activity and projection of optimized dosing design of hydroxychloroquine for the treatment of severe acute respiratory syndrome coronavirus 2 (SARS-CoV-2), *Clin. Infect. Dis.* 71 (2020) 732–739.
- [6] F.O. Shode, A.S.K. Idowu, O.J. Uhomobhi, S. Sabiu, Repurposing drugs and identification of inhibitors of integral proteins (spike protein and main protease) of SARS-CoV-2, *J. Biomol. Struct. Dyn.* (2021) 1–16.
- [7] H. Zhang, J.M. Penninger, Y. Li, N. Zhong, A.S. Slutsky, Angiotensin-converting enzyme 2 (ACE2) as a SARS-CoV-2 receptor: molecular mechanisms and potential therapeutic target, *Intensive Care Med.* 46 (2020) 586–590.
- [8] M. Hoffmann, H. Kleine-Weber, S. Schroeder, N. Krüger, T. Herrler, S. Erichsen, T.S. Schiergens, G. Herrler, N.-H. Wu, A. Nitsche, SARS-CoV-2 cell entry depends on ACE2 and TMPRSS2 and is blocked by a clinically proven protease inhibitor, *Cell* 181 (2020) 271–280.
- [9] R.J. Khan, R.K. Jha, G.M. Amera, M. Jain, E. Singh, A. Pathak, R.P. Singh, J. Muthukumar, A.K. Singh, Targeting SARS-CoV-2: A systematic drug repurposing approach to identify promising inhibitors against 3C-like proteinase and 2'-O-ribose methyltransferase, *J. Biomol. Struct. Dyn.* 39 (2021) 2679–2692.
- [10] Y. Gao, L. Yan, Y. Huang, F. Liu, Y. Zhao, L. Cao, T. Wang, Q. Sun, Z. Ming, L. Zhang, Structure of the RNA-dependent RNA polymerase from COVID-19 virus, *Science* 368 (80) (2020) 779–782.
- [11] C. Wu, Y. Liu, Y. Yang, P. Zhang, W. Zhong, Y. Wang, Q. Wang, Y. Xu, M. Li, X. Li, Analysis of therapeutic targets for SARS-CoV-2 and discovery of potential drugs by computational methods, *Acta Pharm. Sin. B.* 10 (2020) 766–788.

- [12] M. Depfenhart, G. Lemperle, M. Meyer, M. Rautenbach, D. Bertossi, D.A. de Villiers, A SARS-CoV-2 prophylactic and treatment: a counter argument against the sole use of chloroquine, *Am J Biomed Sci Res* 8 (2020) 248–251.
- [13] O.A. Olaleye, M. Kaur, C. Onyenaka, T. Adebuseyi, Discovery of Clloquinol and analogues as novel inhibitors of Severe Acute Respiratory Syndrome Coronavirus 2 infection, ACE2 and ACE2-Spike protein interaction in vitro, *Heliyon* 7 (2021) e06426.
- [14] A. Teimury, E.M. Khaledi, Current options in the treatment of COVID-19: a review, *Risk Manag. Healthc. Policy* 13 (2020) 1999.
- [15] A. Basu, A. Sarkar, U. Maulik, Computational approach for the design of potential spike protein binding natural compounds in SARS-CoV2, (2020).
- [16] D.C. Hall Jr, H.-F. Ji, A search for medications to treat COVID-19 via in silico molecular docking models of the SARS-CoV-2 spike glycoprotein and 3CL protease, *Travel Med. Infect. Dis.* 35 (2020) 101646.
- [17] K. Senathilake, S. Samarakoon, K. Tennekoon, Virtual screening of inhibitors against spike glycoprotein of 2019 novel corona virus: A drug repurposing approach, (2020).
- [18] V.K. Maurya, S. Kumar, M.L.B. Bhatt, S.K. Saxena, Therapeutic development and drugs for the treatment of COVID-19, *Coronavirus* (2020) 109.
- [19] M. Wang, R. Cao, L. Zhang, X. Yang, J. Liu, M. Xu, Z. Shi, Z. Hu, W. Zhong, G. Xiao, Remdesivir and chloroquine effectively inhibit the recently emerged novel coronavirus (2019-nCoV) in vitro, *Cell Res.* 30 (2020) 269–271.
- [20] C. Liu, Q. Zhou, Y. Li, L. V. Garner, S.P. Watkins, L.J. Carter, J. Smoot, A.C. Gregg, A.D. Daniels, S. Jervey, Research and development on therapeutic agents and vaccines for COVID-19 and related human coronavirus diseases, (2020).
- [21] D. Naidoo, V. Maharaj, N.R. Crouch, A. Ngwane, New labdane-type diterpenoids from *Leonotis leonurus* support circumscription of Lamiaceae s.l, *Biochem. Syst. Ecol.* 3 (2011) 216–219.
- [22] K.S. Prabhu, R. Lobo, A.A. Shirwaikar, A. Shirwaikar, *Ocimum gratissimum*: a review of its chemical, pharmacological and ethnomedicinal properties, *Open Complement. Med. J.* (2009) 1.
- [23] N.I. de Melo, C.E. de Carvalho, L. Fracarolli, W.R. Cunha, R.C. Veneziani, C.H. Martins, A.E. Crotti, Antimicrobial activity of the essential oil of *Tetradenia riparia* (Hochst.) Codd. (Lamiaceae) against cariogenic bacteria, *Braz. J. Microbiol.* 46 (2015) 519–525.
- [24] N. Garaniya, A. Bapodra, Ethno botanical and phytopharmacological potential of *Abrus precatorius* L.: a review, *Asian Pac. J. Trop. Biomed.* 4 (2014) S27–S34.
- [25] A. Du Toit, F. Van der Kooy, *Artemisia afra*, a controversial herbal remedy or a treasure trove of new drugs? *J. Ethnopharmacol.* 244 (2019) 112127.
- [26] F.A. Adjé, E.N. Koffi, K.Y. Koné, E. Meudec, A.A. Adima, P.R. Lozano, Y.F. Lozano, E.M. Gaydou, Polyphenol characterization in red beverages of *Carapa procera* (DC) leaf extracts, *Beverages* 5 (2019) 68.
- [27] R.M. Mangoale, A.J. Afolayan, Effects of rhizome length and planting depth on the emergence and growth of *Alepidea amatymbica* Eckl. & Zeyh, *Plants* 9 (2020) 732.
- [28] D.H. Paper, E. Karall, M. Kremser, L. Krenn, Comparison of the antiinflammatory effects of *Drosera rotundifolia* and *Drosera madagascariensis* in the HET-CAM assay, *Phyther. Res. An Int. J. Devoted to Pharmacol. Toxicol. Eval. Nat. Prod. Deriv.* 19 (2005) 323–326.
- [29] W. Yin, C. Mao, X. Luan, D.-D. Shen, Q. Shen, H. Su, X. Wang, F. Zhou, W. Zhao, M. Gao, Structural basis for inhibition of the RNA-dependent RNA polymerase from SARS-CoV-2 by remdesivir, *Science* 368 (80) (2020) 1499–1504.
- [30] Z. Yang, K. Lasker, D. Schneidman-Duhovny, B. Webb, C.C. Huang, E.F. Pettersen, T.D. Goddard, E.C. Meng, A. Sali, T.E. Ferrin, UCSF Chimera, MODELLER, and IMP: an integrated modeling system, *J. Struct. Biol.* 179 (2012) 269–278.
- [31] J. Xu, S. Zhao, T. Teng, A.E. Abdalla, W. Zhu, L. Xie, X. Guo, Syst. Comp. Two Anim. Transm. Hum. Coronaviruses SARS-CoV-2 SARS-CoV, *Viruses*. 12 (2020) 244 n.d..
- [32] M.D. Hanwell, D.E. Curtis, D.C. Lonie, T. Vandermeersch, E. Zurek, G.R. Hutchison, Avogadro: an advanced semantic chemical editor, visualization, and analysis platform, *J. Cheminform.* 4 (2012) 1–17.
- [33] O. Trott, A.J. Olson, AutoDock Vina: improving the speed and accuracy of docking with a new scoring function, efficient optimization, and multithreading, *J. Comput. Chem.* 31 (2010) 455–461.
- [34] I. Kehinde, P. Ramharack, M. Nlooto, M. Gordon, The pharmacokinetic properties of HIV-1 protease inhibitors: a computational perspective on herbal phytochemicals, *Heliyon* 5 (2019) e02565.
- [35] W.L. Jorgensen, J. Chandrasekhar, J.D. Madura, R.W. Impey, M.L. Klein, Comparison of simple potential functions for simulating liquid water, *J. Chem. Phys.* 79 (1983) 926–935.
- [36] J.E. Basconi, M.R. Shirts, Effects of temperature control algorithms on transport properties and kinetics in molecular dynamics simulations, *J. Chem. Theory Comput.* 9 (2013) 2887–2899.
- [37] J.-P. Ryckaert, G. Ciccotti, H.J.C. Berendsen, Numerical integration of the cartesian equations of motion of a system with constraints: molecular dynamics of n-alkanes, *J. Comput. Phys.* 23 (1977) 327–341.
- [38] J.A. Izaguirre, D.P. Catarello, J.M. Wozniak, R.D. Skeel, Langevin stabilization of molecular dynamics, *J. Chem. Phys.* 114 (2001) 2090–2098.
- [39] E. Seifert, OriginPro 9.1: scientific data analysis and graphing software—software review, *J. Chem. Inf. Model.* 54 (2014) 1552.
- [40] M. Ylilauri, O.T. Pentikäinen, MMGBSA as a tool to understand the binding affinities of filamin–peptide interactions, *J. Chem. Inf. Model.* 53 (2013) 2626–2633.
- [41] A. Zumla, J.F.W. Chan, E.I. Azhar, D.S.C. Hui, K.-Y. Yuen, Coronaviruses- drug discovery and therapeutic options, *Nat. Rev. Drug Discov.* 15 (2016) 327–347.
- [42] R. Alexpandi, J.F. De Mesquita, S.K. Pandian, A.V. Ravi, Quinolines-based SARS-CoV-2 3CLpro and RdRp inhibitors and Spike-RBD-ACE2 inhibitor for drug-repurposing against COVID-19: an in silico analysis, *Front. Microbiol.* 11 (2020) 1796.
- [43] R. Islam, M.R. Parves, A.S. Paul, N. Uddin, M.S. Rahman, A. Al Mamun, M.N. Hossain, M.A. Ali, M.A. Halim, A molecular modeling approach to identify effective antiviral phytochemicals against the main protease of SARS-CoV-2, *J. Biomol. Struct. Dyn.* 39 (2021) 3213–3224.
- [44] V.A. Obakachi, N.D. Kushwaha, B. Kushwaha, M.C. Mahlalela, S.R. Shinde, I. Kehinde, R. Karpoornath, Design and synthesis of pyrazolone-based compounds as potent blockers of SARS-CoV-2 viral entry into the host cells, *J. Mol. Struct.* 1241 (2021) 130665.
- [45] Z. Jin, X. Du, Y. Xu, Y. Deng, M. Liu, Y. Zhao, B. Zhang, X. Li, L. Zhang, C. Peng, Structure of M pro from SARS-CoV-2 and discovery of its inhibitors, *Nature* 582 (2020) 289–293.
- [46] S.E.S. John, S. Tomar, S.R. Stauffer, A.D. Mesecar, Targeting zoonotic viruses: Structure-based inhibition of the 3C-like protease from bat coronavirus HKU4—The likely reservoir host to the human coronavirus that causes Middle East Respiratory Syndrome (MERS), *Bioorg. Med. Chem.* 23 (2015) 6036–6048.
- [47] A.T. Jamiu, C.H. Pohl, S. Bello, T. Adedjoja, S. Sabiu, A review on molecular docking analysis of phytochemicals against SARS-CoV-2 druggable targets, *All Life* 14 (2021) 1100–1128, doi:10.1080/26895293.2021.2013327.
- [48] A. Bordogna, A. Pandini, L. Bonati, Predicting the accuracy of protein–ligand docking on homology models, *J. Comput. Chem.* 32 (2011) 81–98.
- [49] M. Hosseini, W. Chen, D. Xiao, C. Wang, Computational molecular docking and virtual screening revealed promising SARS-CoV-2 drugs, *Precis. Clin. Med.* 4 (2021) 1–16.
- [50] T. Sindhu, P. Srinivasan, Exploring the binding properties of agonists interacting with human TGR5 using structural modeling, molecular docking and dynamics simulations, *RSC Adv.* 5 (2015) 14202–14213.
- [51] J.O. Aribisala, S. Nkosi, K. Idowu, I.O. Nurain, G.M. Makolomakwa, F.O. Shode, S. Sabiu, Astaxanthin-mediated bacterial lethality: Evidence from oxidative stress contribution and molecular dynamics simulation, *Oxid. Med. Cell. Longev.* (2021) 24 Article ID 7159652pages, doi:10.1155/2021/7159652.
- [52] J.O. Uhomoihi, F.O. Shode, K.A. Idowu, S. Sabiu, Molecular modelling identification of phytochemicals from selected African botanicals as promising therapeutics against druggable human host cell targets of SARS-CoV-2, *J. Mol. Graphics Modell.* 114 (2022), doi:10.1016/j.jmgm.2022.108185.